Indian J Phys (January 2020) 94(1):105–115
https://doi.org/10.1007/s12648-019-01445-3

ORIGINALPAPER

Laser-induced damage threshold study on TiO_2/SiO_2 multilayer reflective coatings

S Kumar[1]*, A Shankar[1], N Kishore[2], C Mukherjee[3,4], R Kamparath[3] and S Thakur[5]

[1]Optical Engineering Division, Department of Physics, GJUS&T, Hisar, Haryana 125001, India

[2]Department of Physics, Central University Mahendergarh, Mahendergarh, Haryana 123029, India

[3]Advanced Laser and Optics Division, Raja Ramanna Centre for Advanced Technology, Indore 452013, India

[4]Homi Bhabha National Institute, Mumbai 400094, India

[5]Applied Spectrocopy Division, Bhabha Atomic Research Centre, Trombay, Mumbai 400 085, India

Received: 27 March 2018 / Accepted: 31 January 2019 / Published online: 9 April 2019

Abstract: Laser-induced damage threshold (LIDT) is a key parameter in high power laser systems. Highly reflective mirrors are made by the combination of high index and low index dielectric thin films of materials, usually oxides, having high damage threshold. The aim of the present investigation was to study the effect of multilayers on LIDT for a combination of high and low index material films with the increase in the number of layers. Firstly, we chose a combination of relatively high damage threshold high index (H) and low index (L) oxide materials, like TiO_2 and SiO_2. Then, we chose five reflective samples with increasing the number of layers starting with a TiO_2 single quarter wave optical thick (QWOT) layer, three-QWOT layer $(HL)^1H$, five-QWOT layer $(HL)^2H$, seven-all QWOT layer $(HL)^3H$ and seven-layer $(HL)^2H$ 1.6L0.4H with upper two non-quarter layers for sample preparation using electron beam deposition. It has been found that LIDT measured at 1064 nm for single layer is large (2.09 J/cm^2), decreases for three layers and remains nearly constant (1.51 J/cm^2) as the number of multilayers increases further. When LIDT is measured at 532 nm, LIDT of the single layer and multilayers remains almost the same. However, in case of top two layers made of non-QWOT in seven-layer design the LIDT of the samples in both the cases improved.

Keywords: Multilayer reflection mirror; Laser-induced damage threshold; Oxide material; Refractive index; Non-quarter

PACS Nos.: 42.62.Cf

1. Introduction

In a number of fields of science and technology, the present day research and development programmes require high power lasers. The damage limit of optical materials and coatings has been proved to be the major factor limiting the output power of any high power laser systems [1]. The failure of optics of the laser cavity is the key hindrance in the path of such research [2, 3], and therefore, laser-induced damage threshold (LIDT) of laser optics is must for the development of high power lasers. LIDT of the optics depends on many factors of the laser beam such as its wavelength, beam spot size, beam shape, pulse width and repetition rate of the pulses in case of pulsed laser as well as deposition parameters [4]. The dependency of LIDT on wavelength is usually given as $\text{LIDT} \propto 1.45\lambda^{0.43}$; however, in short pulse width region of picoseconds and femtoseconds, LIDT dependency on pulse width (τ) is given as $\text{LIDT} \propto \tau^{1/2}$ [4–7].

In the thin film layer deposition for the high power laser coatings, some important factors, such as starting materials, deposition rate, substrate temperature and annealing temperature, have traditionally been adjusted to optimize the control of the optical constant and absorption of the films [3, 8, 9]. "TiO_2 is a hard, durable and laser damage-resistant material with high refractive index and is widely used to produce multilayer coatings in the visible spectral

*Corresponding author, E-mail: sunilkirori@gmail.com

region" [5, 10] as well as in IR region [5, 11]. Surface morphology of HR mirror shows surface defects which are the main cause for damage [8]. The LIDT of 8.7 J/cm^2 is reported at 532 nm wavelength with 8 ns pulse width, and that of 1.2 J/cm^2 is reported at 800 nm wavelength with 220 ps pulse width for TiO_2/SiO_2 HR mirrors [5]. The main three damage mechanisms are thermally induced damage, avalanche ionization and multi-photon ionization [4].

The dielectric material absorbs the laser energy whenever the energy density reaches up to the desired cut-off limit which in turn results into ablation and structural changes in the dielectric specimen. The electric field distribution within the specimen has a significant effect over the rate of various nonlinear phenomena. The more general case showing this effect is in multilayer coatings, where attempts have been taken into, considering the modification of electric field distribution in dielectric specimen in order to enhance the laser-induced damage thresholds (LIDTs). The interface of dielectric materials layer of high and low refractive indices is highly prone to damage, and therefore, it can be considered as the weakest region. Hence, several investigations have been made where it is shown that by shifting the peak electric field value to a region of low refractive index materials, one can reach a limit which is in accordance with the enhancement of LIDT as determined by dielectric properties of the concerned materials [12–14].

The short pulses excite the electrons of wide band gap dielectrics from valance band into conduction band which results into the creation of phonons by the transfer of their energy to the lattice. In this way, damage of dielectrics occurs provided the heat transferred is sufficient to alter the target materials. The critical electron density in the conduction band of $N_{cr} = 10^{16}$–10^{18} cm^{-3} correlates with critical energy density for damage to occur [12, 15].

Earlier workers reported LIDT measurement with different deposition parameters and different pulsed laser parameters. Dependence of LIDT on oxygen partial pressure is reported by Yao et al. [16] and shows that LIDT decreases with decreasing oxygen partial pressure. In another study, Yao et al. [2] give the LIDT of TiO_2/SiO_2 HR mirror at 1064 nm with 12 ns pulse width in one-on-one mode. Ristau et al. [1] reported the LIDT of different oxide materials having band gap of 3.3 eV to 8 eV, and the value of LIDT for femtosecond laser pulse obtained in TiO_2 thin film is 0.5 J/cm^2 for 100 fs pulse. Jiao et al. [11] studied the TiO_2/SiO_2 high reflecting mirrors prepared by e-beam deposition and measured LIDT with Q-switched laser at 1064 nm wavelength with 10 ns pulse at incident angle of 45° obtaining the value of LIDT 9.5 J/cm^2 [11]. In all such LIDT studies on TiO_2/SiO_2 multilayers, no report on the effect of varying few layers from QWOT to non-QWOT is given. In the present work, laser-induced damage threshold of single layer of TiO_2 and multilayers of TiO_2/SiO_2 with successively increasing numbers of layers in high reflector is investigated. Variations in LIDT from single layer to multilayer with two outer non-QWOT layers are studied at two different laser wavelengths (532 nm and 1064 nm). Transmission/reflection spectra are recorded, and band gap of thin film materials is estimated. Standing wave electric field of laser light is calculated which shed light on the LIDT mechanism of the films.

2. Experimental details

During the present study, we prepared samples of reflective coating using the combination of high index (H) material TiO_2 together with low index (L) material SiO_2, starting with a single quarter wave optical thick (QWOT) layer to successively increasing the number of layers to form multilayers. The samples with three-layer $(HL)^1H$, five-layer $(HL)^2H$, seven-all quarter layer $(HL)^3H$ and seven-layer $(HL)^2H$ 1.6L0.4H with upper two non-quarter layers were deposited on BK7 substrate by e-beam deposition method on box type coating plant (model BC-600 Hind High Vacuum) where we used Argon gas for glow discharge cleaning. Initially, the chamber is pumped till pressure of 5×10^{-5} mbar is achieved. Then, argon gas were supplied inside the chamber (10–20 sccm) till the vacuum is down to 2×10^{-2} mbar desired for glow discharge. Then, discharge was created in the chamber by applying high voltage of 0.5 kV and increasing the current up to 100 mA and glow discharge continued for 10 min. Typical Ar+ ion energies are in the range 20 to 100 eV. Using gradient heater, substrate temperature kept at of 220 °C and oxides were deposited under partial pressure of oxygen gas maintained in the chamber as 3.5×10^{-4} mbar during TiO_2 material deposition and as 3×10^{-4} mbar for SiO_2 material deposition. The evaporation rate was maintained between 1 and 1.5 Å/s for TiO_2 and between 3 and 5 Å/s for SiO_2 layer depositions. Evaporation process parameters were maintained till the thickness of 56.62 nm for TiO_2 and 102.16 nm for SiO_2 (single quarter wave optical thickness) was achieved for the films. After cooling down the chamber, samples were taken out for characterization. Similarly other samples were prepared as per the number of layers required and the desired sequence of layers and its thickness.

Grazing Incidence X-ray Diffraction (GIXRD) and X-ray Reflectivity (XRR) patterns of samples are taken with a Bruker (D8 Discover) instrument. The samples were characterized by GIXRD with 2θ angle in the range of 20° to 80° using steps of 0.039655°, and X-ray reflectivity of TiO_2 thin film is measured from 2θ in the range 0.2° to 4°. Reflection and transmission of all the samples have been

measured with Carry-5000 spectrophotometer. Using spectrometer data, band gap of TiO_2 is calculated. Ellipsometric studies of the samples were performed with the ellipsometer (model SOPRA GES-5), and measurements were achieved with an average value of incident angle about 70° in a wavelength range of 200 to 800 nm at ambient temperature, and data so received were analysed in professional software Winelli II to compute film thickness and refractive index of the film. Laser-induced damage threshold of the samples is measured using Nd:YAG laser having wavelength 1064 nm, 10 ns pulse width and 1 Hz repetition rate. Beam diameter of the laser used was 10 mm, and a lens of focal length 300 mm was used to focus the laser beam. LIDT of single-layer TiO_2 and TiO_2/SiO_2 HR testing was performed with 10 shots of same energy density on a single point. Energy density increased by displacing sample towards the focus point from the lens till the damage occurs. The morphology of the film samples in single layer as well as in multilayers before damage is studied by Atomic Force Microscopy (AFM) technique to evaluate the roughness of the surface that is used in studying the scattering loss. Surface topography of thin film samples was imaged using a multimode scanning probe microscope (NT-MDT, SOLVER-PRO, Russia). AFM measurements were carried out in a non-contact mode using silicon cantilever tips having radius of curvature of $\sim$ 20 nm and a spring constant of 5.5 N/m at resonance frequency of 170 kHz under ambient conditions. Top of the sample surface is always electrically grounded to avoid accumulation of static charge on such dielectric samples. Raster scan rate is 1 Hz with the number of lines 512. Scanning Electron Micrograph of the samples was taken with an electron microscope (SEM), consisting of electron optical system and the specimen, which must be kept at a very high vacuum of 10^{-3} to 10^{-4} pa; accelerating voltage for thermo electrons should be 1 to 30 kV as secondary electron needs to be ejected from the surface of the specimen. Furthermore, in order to avoid the charge-up effect on the surface, the sample (specimen) needs to be conducting in nature, but for non-conducting samples, it needs to be coated with some noble metal like Au, Pt, etc. An electron microscope (SEM) [Model MIRA3 TESCAN] system was used to study surface morphology and to investigate the probable damage mechanism in the films.

3. Results and discussion

3.1. Grazing incidence X-ray diffraction (GIXRD) and X-ray reflectivity (XRR)

X-ray diffraction patterns of TiO_2 single layer and SiO_2 single layer are shown in Fig. 1. Multilayers of TiO_2/SiO_2 (HR mirror) are deposited in the same environment as single-layer TiO_2 and SiO_2. X-ray diffraction patterns have been used to investigate the phase of the prepared TiO_2 thin films. In the X-ray diffraction pattern, there is no sharp peaks present, but a broad hump in the low 2θ (22°) region is shown for as deposited films and also in samples annealed at low temperature ($\leq$ 300 °C) which indicate the amorphous nature of samples [17]. In case of SiO_2 also, the absence of any sharp peak confirms the amorphous nature of film. The amorphous phase of SiO_2 depicts the absence of grains in the grown film.

X-ray reflectivity plot of TiO_2 thin film shows the normalized intensity as a function of momentum component Q_z [18] where Q_z is given by

$$Q_z = \frac{4\pi \mathrm{Sin}\theta}{\lambda} \tag{1}$$

where θ is half of the angle 2θ and λ is the wavelength of X-ray used in experiment. Using Parratt formalism [19], experimental data are fitted with a 1.2 nm surface roughness, 0.5 nm interface roughness and 3.06 g/cm^3 film density. The critical angle of the film at which reflection of the X-ray decreases sharply is related to density [20] and is given by

$$\theta_c = \sqrt{\frac{r_0\lambda^2}{\pi}\rho} \tag{2}$$

where r_0 is the Bohr radius, λ is the wavelength of the X-ray, ρ is the density in the film and obtained critical angle for TiO_2 film is 0.55×10^{-2} rad or 0.32°.

From the XRR data, it is seen that there is good contrast of electron density between film and substrate as shown in Fig. 2. At $Z = 0$, there is no sharp increase in the value of rho as there is some roughness on the surface. At film substrate interface also there is some roughness as there is no sharp decrease in the electron density. So both the surfaces have some roughness.

3.2. Optical properties

Reflection and transmission spectra of single TiO_2 layer and TiO_2/SiO_2 multilayers with successive increasing the number of layers are shown in Fig. 3. Peak reflectivity of single TiO_2 layer achieved is about 27.2%, i.e., most of the incident light gets transmitted (above 70% as shown in Fig. 3) from this coating which is the conformity with the amorphous nature of the deposited film [17]. Reflectivity for TiO_2/SiO_2 three layers is 56.2%, for TiO_2/SiO_2 five layers is 76.1%, for TiO_2/SiO_2 seven layers is 86.6% and reflectivity for TiO_2/SiO_2 seven layers with last two layers are non-QWOT is 81.9%. It is evident and expected that reflectivity of these samples increases with the number of

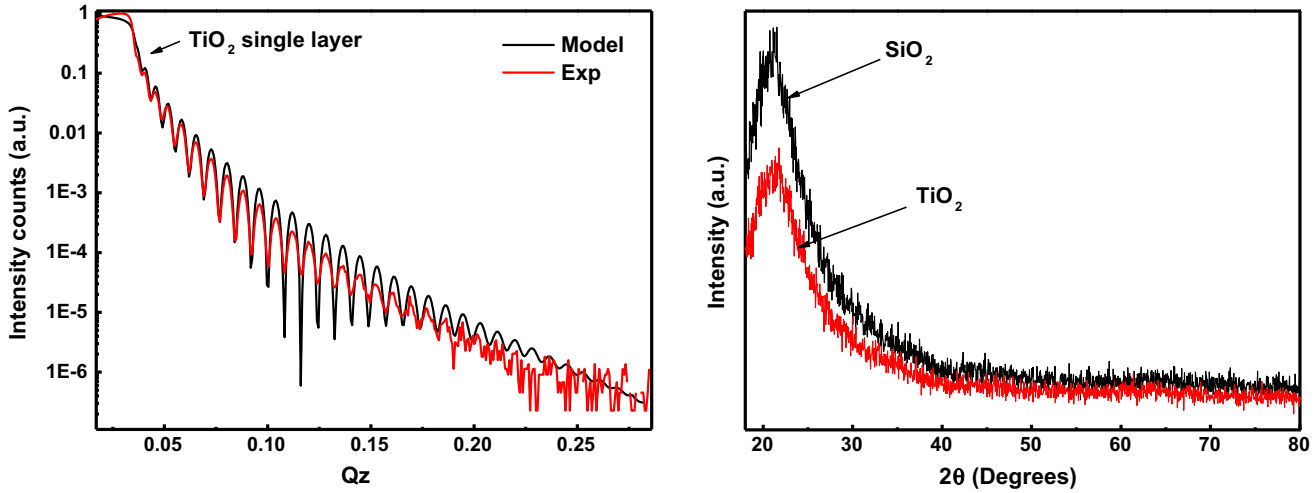

Fig. 1 X-ray reflectivity curve of TiO_2 single-layer film (experimental and fitted) and GIXRD graph of SiO_2 and TiO_2 single layer

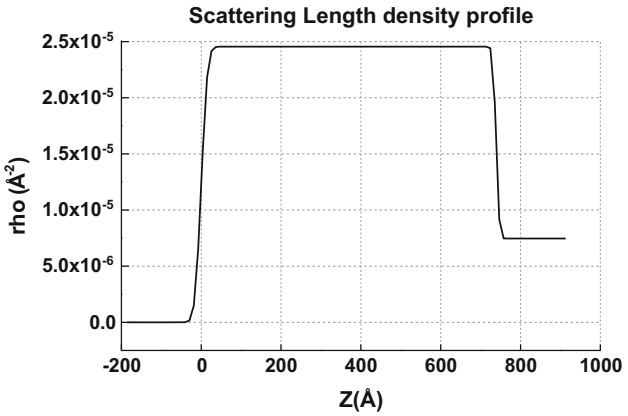

Fig. 2 Density profile of TiO_2 thin film on SiO_2 substrate

layers. Reflectivity of TiO_2/SiO_2 multilayers with last two layers non-quarter wave thickness is less than that of equivalent multilayers with all quarter wave design thin films, but laser damage threshold is higher in non-quarter wave thickness sample. Hence, we adopt this peak shift method for developing high damage threshold mirror.

3.3. Band gap

The optical band gap of TiO_2 and SiO_2 thin films was determined by Tauc plot of α^2 versus $h\upsilon$ based on the following equation [17, 21]:

$$(\alpha h\upsilon)^2 = B\,(h\upsilon - E_g) \tag{3}$$

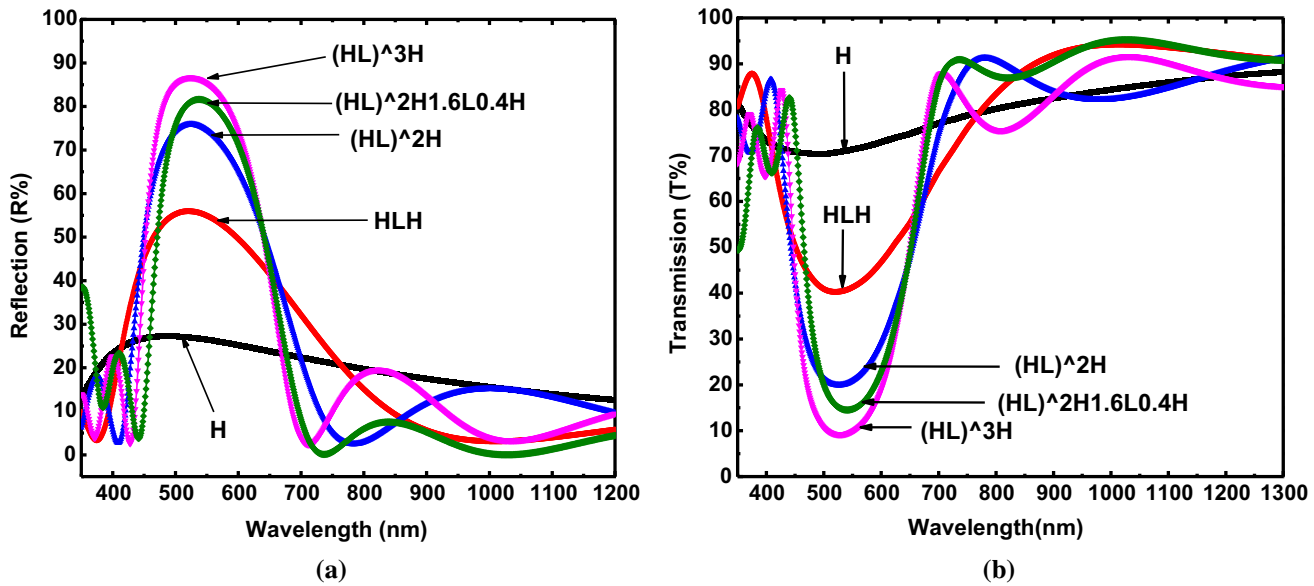

Fig. 3 Reflection and transmission of TiO_2 and TiO_2/SiO_2 multilayer samples at 532 nm wavelength

where α is the absorption coefficient, $h\nu$ the incident photon energy, E_g the optical band gap energy and B a constant. The optical band gap values so obtained were of the order of 3.9 eV, which are in good agreement with those reported by Govindasamy et al. [22]. LIDT of the samples is also explained on the basis of band gap. Higher band gap dielectrics have high damage threshold. As the material TiO_2 used for the HR coating has comparatively lower band gap than the SiO_2 (Fig. 4), hence, LIDT of SiO_2 is higher, which is used to improve the LIDT of non-quarter multilayers by shifting the peak of electric field from interface of TiO_2/SiO_2 to SiO_2 material layer.

3.4. Ellipsometric results

Ellipsometry uses the fact that light undergoes some change in polarization when it is reflected from the surface of a sample. The change in polarization is due to the surface structure of the sample [23]. The film thickness and other optical constants are estimated using Cauchy dispersion relation [24] as given in Eqs. 4 and 5.

$$n(\lambda) = A + \frac{B}{\lambda^2} + \frac{C}{\lambda^4} + \tag{4}$$

$$k(\lambda) = D + \frac{E}{\lambda} + \frac{F}{\lambda^3} + \tag{5}$$

Simulated and experimental results of ellipsometry are shown in Fig. 6. A model layer to simulate the surface roughness was included at the air–film interface as shown in Fig. 5. The model given in Fig. 5 is the samples of single layer of TiO_2 and SiO_2. In the case of TiO_2 single layer, a film of thickness 56.6 nm is deposited over which there is a roughness of 2.7 nm, i.e., if a second layer is deposited then there is interdiffusion of material up to this limit. Similarly in thin film of SiO_2, the thickness is 102.2 nm over which a rough layer of 6.7 nm is observed. The film structures were simulated with root mean squared errors (RMS) values [25]. So we obtained a number of information such as film thickness, refractive index (n) extinction coefficient (k) about the sample material simply by analysing the reflected light beam using ellipsometry [20]. The simulated results are shown in Table 1.

The variation in refractive index (n) and extinction coefficient (k) with wavelength is shown in Fig. 7(a) and (b).

Refractive index of thin film found at 532 nm is 2.1 for TiO_2 film and 1.43 for SiO_2; extinction coefficient is 1.5×10^{-2} and 2.02×10^{-3} for TiO_2 and SiO_2 material, respectively. In nanosecond regime, absorption in thin film is responsible for the damage which depends on extinction coefficient (k); larger the k value, the lower is the LIDT of coating.

3.5. Atomic force microscope (AFM)

The surface topography of films is shown in Fig. 8(a)–(f). The surfaces of the coatings were scanned using an AFM with a scan size of 2 μm × 2 μm. All the samples are prepared at 220 °C substrate temperature, and all are amorphous in nature. The root mean square (RMS) roughness of SiO_2 single layer is 0.51 nm, and it is 0.33 nm for TiO_2 single layer. In multilayer high reflector TiO_2/SiO_2 seven layers, the RMS roughness increases to 0.64 nm, slightly larger than single layers [26, 27] as determined from AFM data. Figure 8(a), (b) shows the 2D and 3D view of SiO_2 single layer. Figure 8(c), (d) shows the 2D and 3D view of TiO_2 single layer. Columnar morphology is shown in Fig. 8(a), (b). TiO_2 films (Fig. 8c, d)

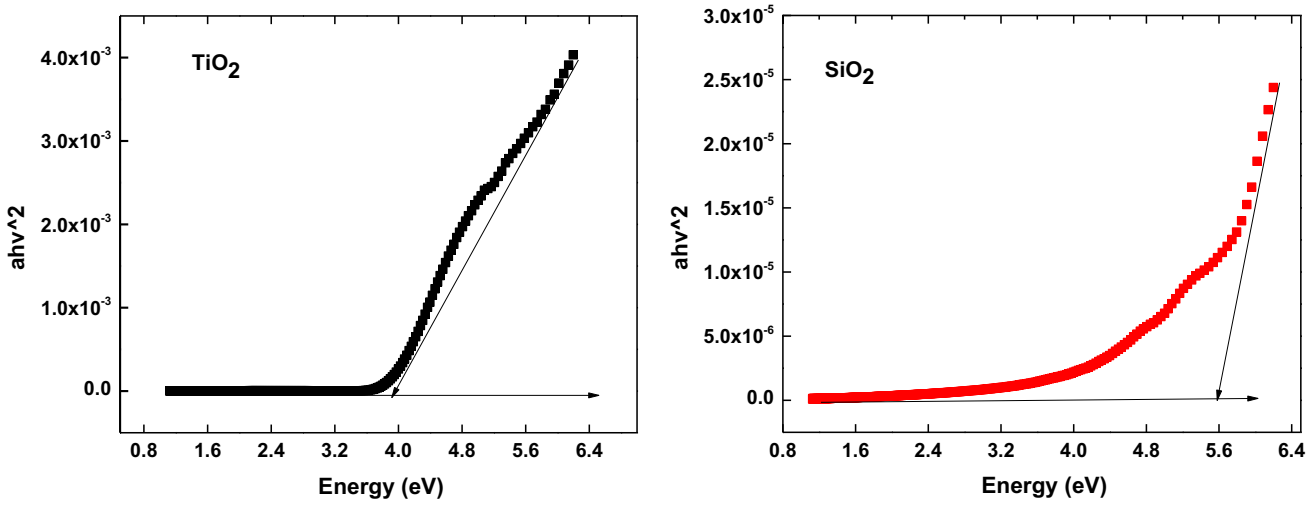

Fig. 4 Graph for the calculation of band gap of TiO_2 and SiO_2 thin film

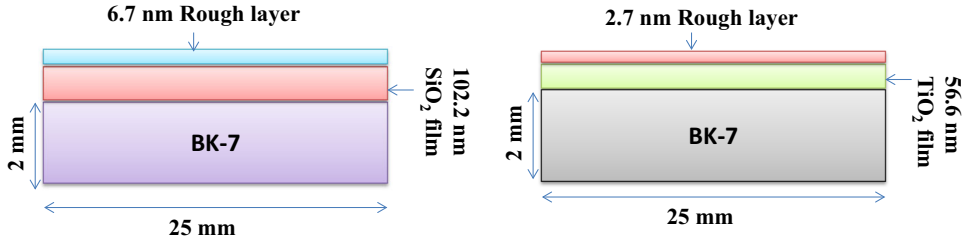

Fig. 5 Model of SiO_2 and TiO_2 for ellipsometric measurement

Table 1 Results of ellipsometry

Parameters	SiO_2	TiO_2
Thickness (nm)	102.2 ± 1.6	56.6 ± 1.2
Roughness (nm)	6.7 ± 0.8	2.7 ± 0.4
Refractive index	1.43	2.1
Extinction coefficient	2.02×10^{-3}	1.5×10^{-2}

are much smoother than SiO_2 film. Figure 8(e), (f) shows that when TiO_2 is grown above SiO_2 layer, roughness is larger than in the individual films. As roughness increases, scattering loss also increases and very high reflectivity cannot be achieved. Additionally, scattering points on films lower laser-induced damage threshold.

3.6. Scanning electron microscope (SEM)

The unclear edge of damage crater suggests that the thermal damage mechanism and heat diffusion play an important role. Damaged sites are centred on one or more absorption points, which are attributed to the existence of defects [16]. When laser radiation is incident on TiO_2 single layer, film is melted and left a large damaged area as shown in Fig. 9(a) and (b). In multilayer (HL)^3H thin film, at the bottom of the pits, no damage precursors are visible as shown in Fig. 9(c) and (d); invisible absorbing centres were the probable cause of damage in TiO_2/SiO_2 multilayer coating. In the HR coating, the absorbing centres in these layers, especially in interface, are more prone to induce laser damage. The material surrounding the absorber can be melted or fractured off by the laser irradiation on these absorbing centres.

3.7. Laser damage threshold

Measured LIDT of these samples is given in Table 2. The nanosecond laser-induced damage of HR mirror is initiated by the absorption of laser energy induced by different defects, such as the atomic non-stoichiometric defects, impurities and other nanometre absorbing defects. As a result of atomic non-stoichiometric defect, intrinsic absorption of laser energy occurs and shows SEM micrograph which is different from that of impurities and other nanometric defects. Impurity defects arise due to impure material or contaminated chamber, and other nanometric absorbing defects arise due to manufacturing

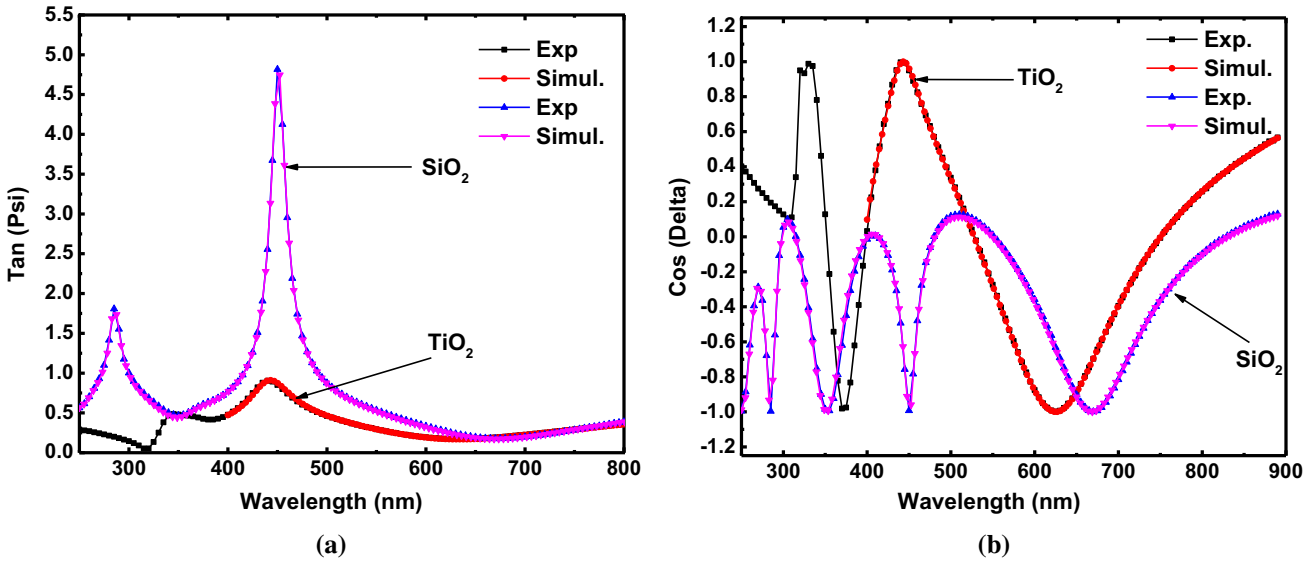

Fig. 6 Experimental and simulated results of ellipsometry

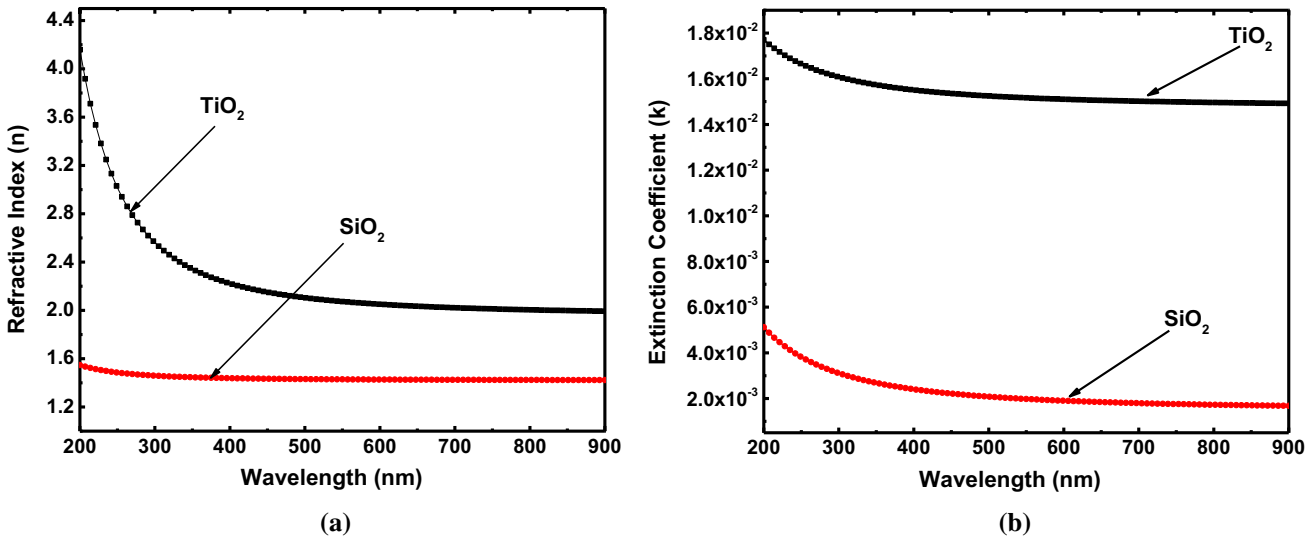

Fig. 7 Variation in refractive index (**a**) and extinction coefficient (**b**) with wavelength

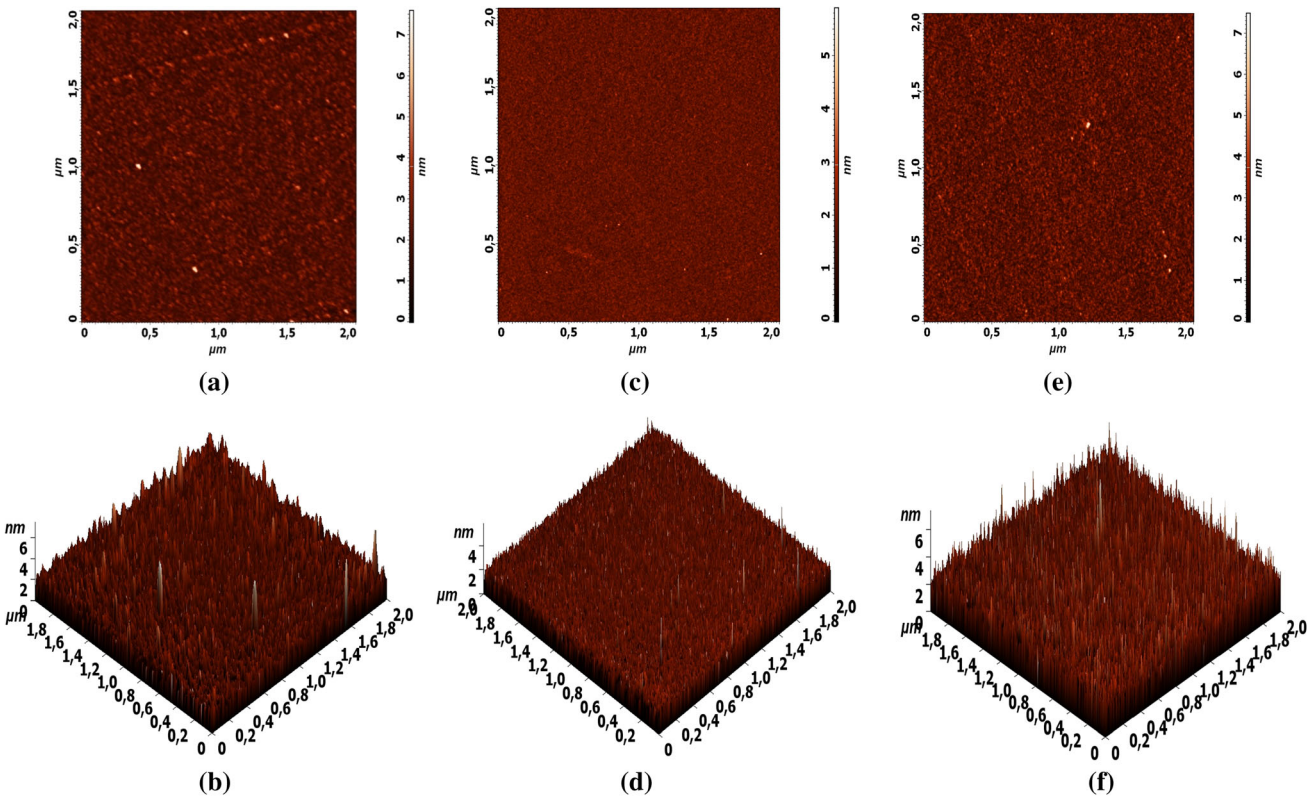

Fig. 8 2D and 3D view of surface topography of SiO_2 film (**a**, **b**) and TiO_2 film in (**c**, **d**) and TiO_2/SiO_2 multilayer in (**e**, **f**)

process (cleaning, polishing and during the formation of thin film). SEM micrographs of impurity defects have cracks and fractures, and nanometric defect SEM micrograph shows the pit formation. In the present study, SEM image of the damaged samples shows that the damage is initiated at the point where energy-absorbing centres are present. These energy-absorbing centres are called defects in the thin film. More energy of incident laser light is absorbed by these defects compared to the surroundings, and the damage occurs. Slightly absorbing TiO_2/SiO_2 HR mirrors have low damage fluence 1.43 ± 0.07 J/cm^2 and 1.51 ± 0.07 J/cm^2 at 532 nm and 1064 nm, which are probably due to low band gap energy and high absorption [28].

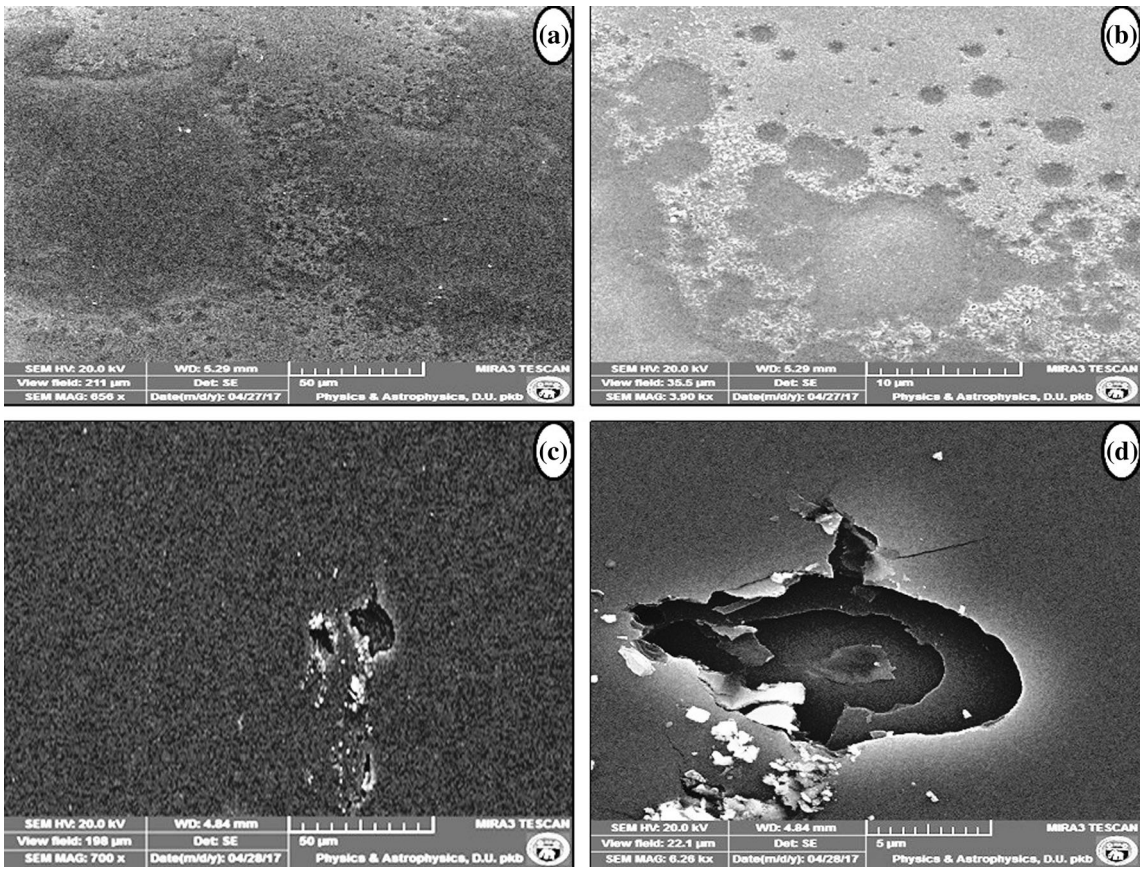

Fig. 9 SEM images of damage morphology in thin film

Table 2 LIDT of TiO_2 single layer and different multilayer high reflective mirrors

Sample	LIDT (J/cm^2) @532 nm	LIDT (J/cm^2) @1064 nm
H	1.43 ± 0.07	2.09 ± 0.09
HLH	1.43 ± 0.07	1.51 ± 0.07
$(HL)^2$ H	1.43 ± 0.07	1.51 ± 0.07
H $(HL)^3$	1.43 ± 0.07	1.51 ± 0.07
$(HL)^2$H1.6L0.4H	1.63 ± 0.08	2.09 ± 0.09

LIDT of single TiO_2 layer is 1.43 ± 0.07 J/cm^2 for 532 nm and is 2.09 ± 0.09 J/cm^2 for 1064 nm, and that of TiO_2/SiO_2 HR with upper two layers non-quarter wave thickness is 1.63 ± 0.08 J/cm^2 and 2.09 ± 0.09 m J/cm^2 for 532 nm wavelength and 1064 nm wavelength, respectively, in nanosecond pulse width range. Uncertainty in laser damage threshold is due to the following: pulse-to-pulse energy variation, pulse-to-pulse width variation and pulse-to-pulse spot size variation at the sample surface.

From the data presented in Table 2, it may be seen that LIDT of single-layer TiO_2 and multilayer TiO_2/SiO_2 in all quarter wave thicknesses remains the same at 532 nm wavelength. This is because at this wavelength interface effect in multilayers is negligible and absorption due to defects and impurity is dominating which are the same in single as well as multilayers with all quarter wave thicknesses. LIDT at 1064 nm wavelength for single-layer TiO_2 is higher and decreases for multilayers of TiO_2/SiO_2 in all quarter wave thickness samples. This is due to reason that at this wavelength the interface effect is more pronounced and peak electric field which lies on interface is responsible for the decrease in the LIDT value. Further LIDT increases in non-quarter wave design samples at both 532 nm and 1064 nm wavelengths due to shifting of the peak from interface due to high damage reason. Damage morphology of the TiO_2 single layer and TiO_2/SiO_2 HR is shown as SEM images in Fig. 9.

3.8. Electric field

Electric fields of these samples were estimated by thin film design software TFcalc and are shown in Fig. 10(a)–(j). Electric field generated because of incidence of laser light on the thin films is responsible for damage produced due to avalanche ionization. Electrons already present in the conduction band absorb energy from photons emitted by laser light and transfer this energy to electron in valence

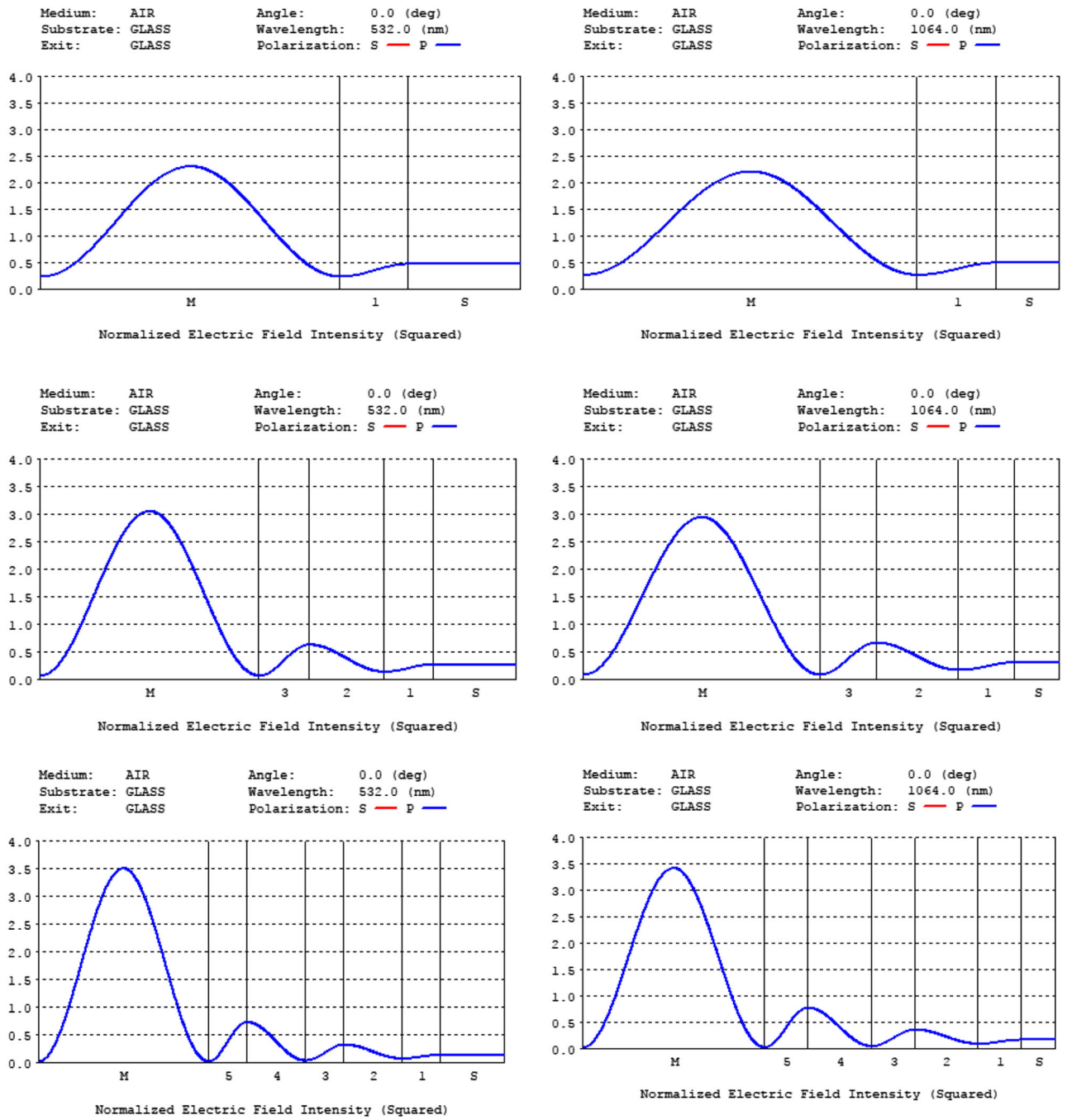

Fig. 10 Electric field distribution of TiO_2 and TiO_2/SiO_2 different multilayer films

band, and these valence band electrons are excited into the conduction band. As the electron density reaches $N_{cr} = 10^{16}$–10^{18} cm^{-3}, damage occurs [15]. According to electric field intensity consideration, TiO_2 is a low damage threshold material as compared to SiO_2, because the band gap of SiO_2 is much higher than that of the TiO_2. In multilayer thin films, peak electric field is more damaging at the interface of the high and low index materials and hence reduces the damage threshold. In this study, the peak of electric field is shifted from the interface to low index material or high damage threshold region. Abromavicius et al. [29] report an increase in the damage threshold of HR mirrors by almost a factor of two just by adjusting the layer structure in such a way that the highest occurring electric fields are located in the high band gap material [29]. Electric field value at the incidence face in single-layer TiO_2 is higher than that in multilayers, but LIDT values are the same both for single layer and for multilayers. As the number of layer increases, peak electric field value increases at the first interface of high and low index

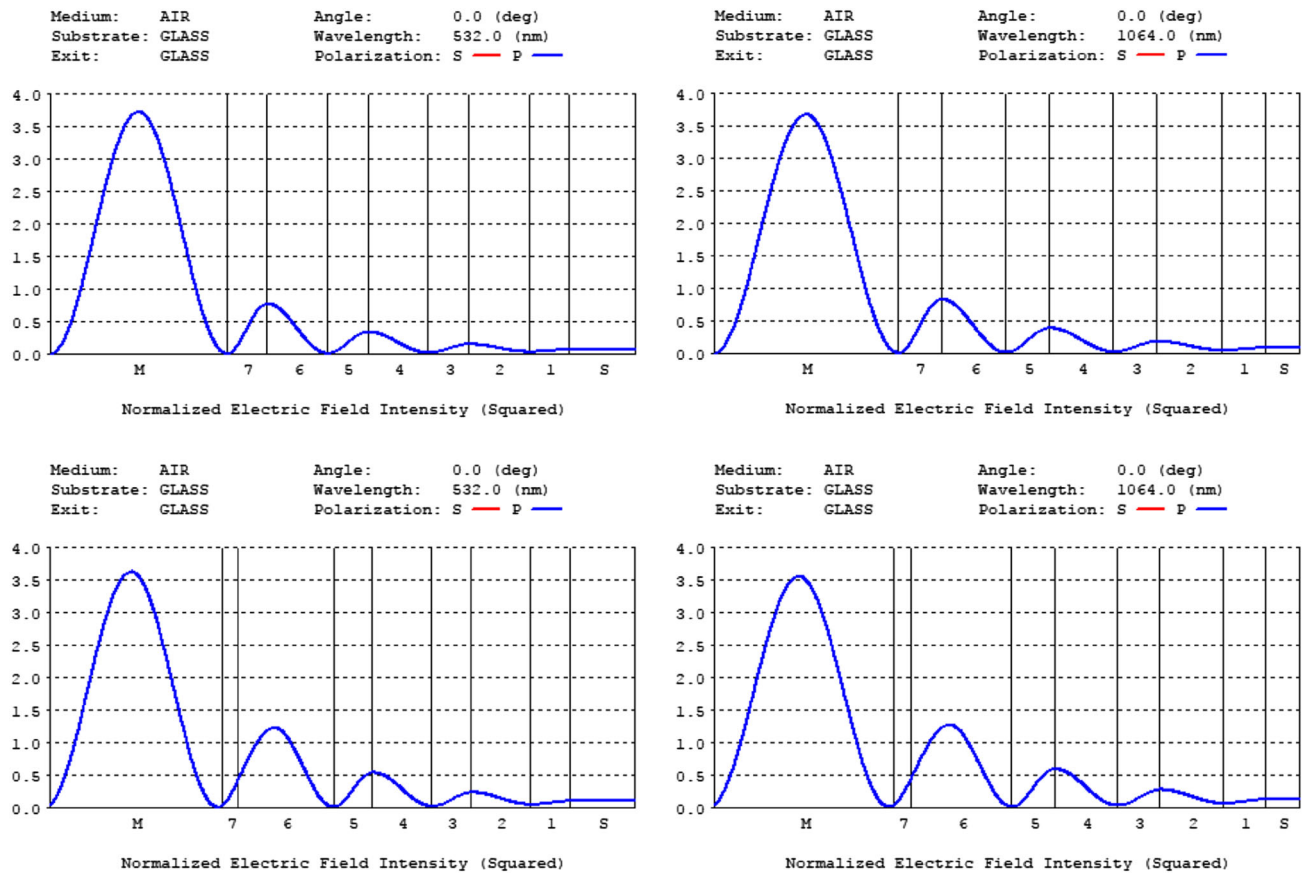

Fig. 10 continued

material as shown in Fig. 10(a), (c), (e) and (g); hence, the decrease in electric field value at incident face is compensated by the increase in electric field at the first interface so LIDT is same for single layer and multilayers for 532 nm wavelength. At wavelength 1064 nm, LIDT of single layer is higher than that of multilayers because in this case, the contribution of the peak electric field value is more dominating than the contribution of incident face electric field value as shown in Fig. 10(b), (d), (f) and (h). In non-quarter wave design, LIDT increases for both wavelengths because of the shifting of peak electric field from first interface to low index material that is the region of high laser damage threshold as shown in Fig. 10(i), (j), and hence, overall damage threshold of multilayer is augmented.

4. Conclusions

Laser-induced damage threshold of single-TiO_2 layer and multilayer TiO_2/SiO_2(with successive increasing layers) is studied, i.e., TiO_2/SiO_2 three layers, TiO_2/SiO_2 five layers, TiO_2/SiO_2 seven layers and TiO_2/SiO_2 seven layers with upper two non-quarter wave thickness. It has been found that LIDT measured at 1064 nm, compared to single QWOT layer of TiO_2, decreases in three layers design but remains the same as layers are further increased in the design. When LIDT is measured at 532 nm, it remains almost the same for single layer and multilayers. However, for top two layers in non-QWOT of seven-layer design the LIDT of the samples in both the cases is increased. In multilayers, LIDT decreases as the number of layer increases because of the interface effect. As the number of interfaces increases, electric field due to laser intensity has significant effect on the laser damage threshold; hence, the damage threshold decreases.

Acknowledgements This work is supported financially by University Grant Commission, New Delhi, under Basic Science Research (BSR) fellowship. The authors thank Ashok Bhakar, RRCAT Indore and M/s Light Guide Optics for allowing us to use their deposition facility. Funding was provided by UGC-BSR (Grant No. 7-179/2007(BSR)).

References

[1] D Ristau, M Jupen and K Starke *Thin Solid Films* **518** 1607 (2009)
[2] J Yao, J Ma, C Xiu, Z Fan, Y Jin, Y Zhao et al. *J. Appl. Phys.* **103** 083103 (2008)

[3] Y Jian, J Yun, Z Yuan, H Hong, S Jian and F Zheng *Chin. Phys. Lett.* **24** 2606 (2007)
[4] R M Wood Laser-induced damage of optical material *Inst. Phys.* **0 7503 0845 1** 54 (2003)
[5] J Yao, Z Fan, Y Jin, Y Zhao, H He and J Shao *Thin Solid Films* **516** 1237 (2007)
[6] K Yoshida and N Umemura *Proc. SPIE Int. Soc. Opt. Eng.* **164** 3244 (1998)
[7] B Stuart, M Feit, S Herman, A Rubenchik, B Shore and M Perry *Phys. Rev. Lett.* **74** 2248 (1995)
[8] J Yao, H Li, Z Fan, Y Tang, Y Jin, Y Zhao et al. *Chin. Phys. Lett.* **24** 1964 (2007)
[9] K N Rao *Opt. Eng.* **41** 2357 (2002)
[10] J Yao, Z Fan, H He and J Shao *Chin. Opt. Lett.* **5**556 (2007)
[11] H Jiao, T Ding and Q Zhang *Opt. Express* **19** 4059 (2011)
[12] S Kumar, Kamal, A Shankar, N Kishore *J. Integr. Sci. Technol.* **5**5 (2017)
[13] S Chen, M Zhu, D Li, H He, Y Zhao, J Shao et al. *Proc. SPIE* **7842** (2010)
[14] J H Apfel *Appl. Opt.* **16** 1880 (1977)
[15] V Conta Bachelor thesis *Faculty of Precision and Micro Engineering/Engineering Physics University Munich Germany* (2010)
[16] J Yao, Z Fan, Y Jin, Y Zhao, H He and J Shao *J. Appl. Phys.* **102** 063105 (2007)
[17] A Taherniya and D Raoufi *Semicond. Sci. Technol.* **31** 125012 (2016)
[18] J D Paul Whiteside, J A Chininis and H K Hunt *Coat. MDPI* **6** 35 (2016)
[19] The Manual of the Reflectivity Tool, Parratt 32, ETH Zurich
[20] C K Saw, W K Grant, J Stanford, L N Dinh *LLNL-TR* **680742** (2016)
[21] J Tauc *Mater. Res. Bull.* **3** 37 (2007)
[22] G Govindasamy, P Murugasen and S Sagadevan *Mater. Res.* **19** 413 (2016)
[23] http://www.sun-way.com.tw/Files/DownloadFile/Ellipsometry_basics.pdf.
[24] Guide to using WVASE spectroscopic ellipsometry data Acquisition and Analysis software *J A Woollam Co. Inc. Lincoln* NE 68508
[25] S Kohli, C D Rithner and P K Dorhout *Rev. Sci. Instrum.* **76** 023906 (2005)
[26] H Jiao, X Cheng, J Lu, G Bao, Y Liu, B Ma et al. *Appl. Opt.* **50** C309 (2011)
[27] C Xu, Y Qiang, Y Zhu, J Shao, Z Fan *J. Optoelectron. Adv. Mater.* 11 863 (2009)
[28] H Jiao, T Ding and Q Zhang *Opt. Express* **19** 4059 (2011)
[29] G Abromavicius, R Buzelis, R Drazdys, A Melninkaitis and V Sirutkaitis *Proc. SPIE* **6720** 67200Y (2007)